

Brewster angle spectroscopy: A new method for characterization of defect levels in semiconductors

H. J. Lewerenz and N. Dietz

Hahn-Meitner-Institut, Bereich Photochemische Energiewandlung, Postfach 39 01 28, Glienicker Strasse 100, D-1000 Berlin 39, Germany

(Received 15 April 1991; accepted for publication 19 June 1991)

A new optical method which allows the identification of electronic defects in semiconductors is presented. Deep level characterization is done by detecting changes of the Brewster angle induced by optically excited transitions involving defects. An empirical model is developed which correlates the minima of the derivative of the Brewster angle as a function of photon energy with the energetic locations of defects in the semiconductor gap.

Contactless room-temperature measurements on *n*-GaAs (100) and *p*-InP (111) clearly reveal defects with high accuracy, including the well known EL2 and EL12 centers in GaAs. The applicability of the method for semiconductor device technology processes is discussed.

The analysis of electronic defects is of crucial importance for semiconductor materials development. The need for deep level characterization in electronic devices and their components has led to the establishment of a series of detection methods. Among those, techniques such as deep level transient spectroscopy (DLTS),¹⁻⁴ phot capacitance spectroscopy (PCS),⁵⁻⁷ electroreflectance (ER)^{8,9} and photoluminescence (PL)^{5,10} require either sample contacting or cooling. Other methods as, for instance, electron spin resonance (ESR),¹¹⁻¹³ photorefectance,¹⁴ photothermal deflection spectroscopy¹⁵ and standard reflectivity measurements are limited in sensitivity and/or applicability.

The technique presented here is based on the optical properties of semiconductors below the band-gap energy. If, in a first approximation, the semiconductor is viewed as a dielectric in this energy range, the reflectivity for light polarized parallel to the plane of incidence should vanish. The presence of an absorbing defect can be mathematically modeled as a harmonic oscillator, influencing the reflectivity R_p and the Brewster angle ϕ_B . The calculation performed below shows that for a given oscillator strength, the changes in ϕ_B are larger than in R_p . Therefore, a measurement of ϕ_B versus photon energy is characterized by a higher sensitivity.

The influence of an absorbing center on R_p and ϕ_B can be calculated assuming Lorentz oscillatory behavior.^{16,17} For the complex dielectric constant

$$\bar{\epsilon} = \epsilon_1 - i\epsilon_2 = \epsilon_\infty + \sum_i \frac{s_i}{\omega_i^2 - \omega^2 + i\omega\Gamma_i} \quad (1)$$

where ω_i : frequencies of the absorbing centers; Γ_i : damping; s_i : oscillator strength; the Brewster angle can be determined analytically and is described by the function $\phi_B = \arcsin(f(\epsilon_1, \epsilon_2))$ which will be given in the appendix. For comparison of the change in ϕ_B and the change in R_p , we also give the analytical relationship of $R_p = R_p(\epsilon_1, \epsilon_2, \phi)$ in the Appendix.

Figure 1 shows data obtained by incorporation of a simulated defect in a semiconductor band tail region. The data were calculated using several Lorentz oscillators at

$E_g = 1.56$ eV (band gap) and above to simulate typical semiconductor behavior such as for GaAs. A small oscillator (defect center) with an oscillator strength $s_i = 5 \times 10^{-5}$ and a damping of $\Gamma_i = 50$ meV at 0.75 eV

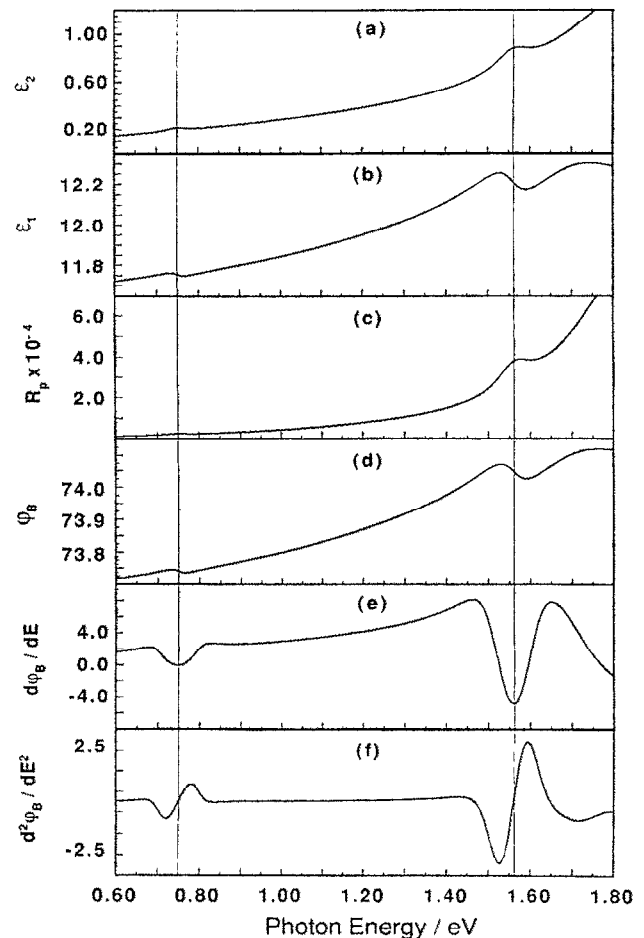


FIG. 1. Calculated optical properties for a simulated dielectric function ϵ generated by Lorentz oscillators. The contribution from oscillators at $\hbar\omega = 1.56$ eV and above simulates the optical properties of a semiconductor with an energy gap at 1.56 eV. A small oscillator at 0.75 eV is used to simulate an optical absorption center within the band gap (a,b); c: reflectivity calculated from Eq. (3); d: ϕ_B calculated from Eq. (2); e,f: first and second derivative of ϕ_B respectively.

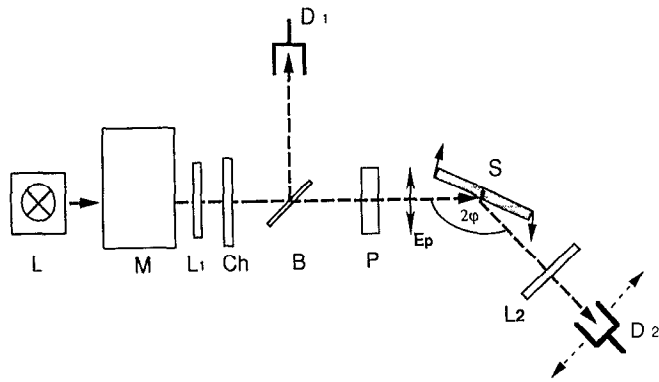


FIG. 2. Schematic drawing of the experimental setup; L: lamp; M: monochromator; L₁, L₂: lenses; Ch: chopper; B: beamsplitter; P: polarizer; D₁, D₂: detectors; S: sample.

has been added. This absorbing center changes the reflectivity at normal incidence R_0 by $\sim 2 \times 10^{-4}$, the real and imaginary part of the dielectric function by $\Delta\epsilon_1 \sim 2 \times 10^{-2}$ and by $\Delta\epsilon_2 \sim 8 \times 10^{-3}$, respectively. The Brewster angle changes by $\Delta\phi_B \sim 1 \times 10^{-2}$ deg and the reflectivity in the minimum by $\Delta R_p \sim 2 \times 10^{-6}$. The assumed defect structure exhibits an oscillator strength which is lower by a factor of ~ 100 compared to the oscillator simulating the onset of direct transitions.

The defect contribution is assumed to be almost undetectable in the ϵ_2 spectrum [Fig. 1(a)]. The calculation shows that the minimum of $d\phi_B/dE_{ph}$ reveals the energetic position of the defect level at 0.75 eV. For higher detection sensitivity, we suggest to use the second derivative $d^2\phi_B/dE_{ph}^2$ where the inflection point identifies the defect level position E_0 [Figs. 1(e) and 1(f)]. The spectral changes in R_p , also displayed in Fig. 1(c) are seen to be smaller than those in ϕ_B [Fig. 1(d)].

The experimental arrangement is schematically shown in Fig. 2. As a light source a tungsten iodine lamp with a Kratos monochromator was used. The light beam is split into a reference and a signal channel, detected at D_1 and D_2 , respectively. The signal beam is polarized parallel to the plane of incidence, using a Glan-Thompson polarizer P . The polarized light is focused onto the sample held at an angle ϕ close to the Brewster angle ϕ_B . The reflected intensity is detected by a cooled Si-(0.4–1 μm) or Ge detector (0.8–1.7 μm). For analysis of the reflected intensity and the Brewster angle position, the signal at D_2 was measured as a function of the angle ϕ . The minimum was determined by a least squares fit and the according reflectivity R_p was determined by comparison with the signal at detector D_1 . Standard lock-in technique was used for data analysis. The accuracy of the method depends critically on the angular resolution of the goniometer table on which the sample is mounted. The mechanical specification yields a resolution better than 2×10^{-3} deg. The step motor limitation results in a resolution of 4×10^{-3} deg. To determine the first and second derivative of the measured Brewster angle spectra a specific algorithm based on a compensation parabola method (quadratic least square fit) was used.¹⁸

In Fig. 3, data recorded on n -GaAs (100) are dis-

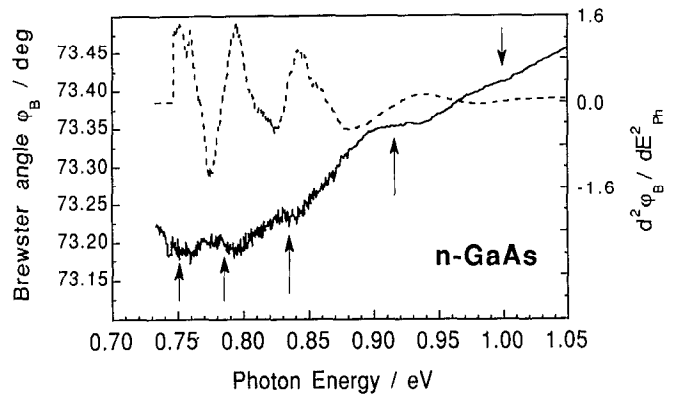


FIG. 3. Spectral dependence of the Brewster angle for n -GaAs; for identification of the defect structures at 0.754, 0.785, 0.835, 0.916, and 1.005 eV, the inflection point of the second derivative and the minima of the first derivative where used.

played. For comparison the spectral dependence of ϕ_B itself is also shown in the figure. The inflection point of the second derivative of the Brewster angle with respect to the photon energy locates the energetic position of a series of levels, among them defects at the energetic position of the well known EL12¹⁹ and EL2^{6,19–21} centers. Additional levels determined by photocapacitance measurements⁶ are also reproduced with high accuracy.

Figure 4 gives an analogous dataset for InP(111). Here, too, the inflection point of $d^2\phi_B/dE_{ph}^2$ determines E_D with high accuracy as evidenced by comparison with literature data.²² It should be noted that two conditions have to be fulfilled simultaneously for unambiguous identification of E_D : inflection of $d^2\phi_B/dE_{ph}^2$ and a minimum in $d\phi_B/dE_{ph}$.

The Brewster angle spectroscopy (BAS) allows the identification of deep levels in the semiconductors and insulators at room temperature. The method is particularly suited in areas where bulk semiconductors have to be analyzed as, for instance, materials preparation for photovoltaics and photoelectrochemistry. The limitations of the method with respect to number and/or concentration of absorbing centers cannot be estimated at present but it

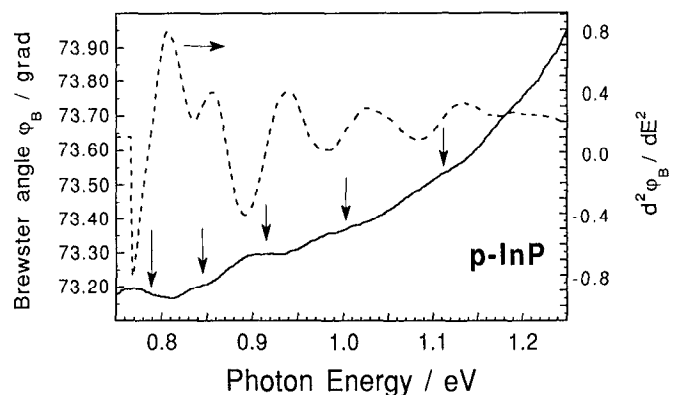


FIG. 4. Spectral dependence of the Brewster angle for InP showing absorbing centers at 0.787, 0.845, 0.916, 1.005, and 1.107 eV; identification of defect level as in Fig. 3.

appears that the sensitivity is among the highest compared to other deep level detection experiments. For development of semiconductor materials for photosensitive devices such as solar cells and detectors, BAS provides a powerful tool in the materials optimization process.

Appendix: The analytical expression for the Brewster angle in the case of a complex dielectric function²³ is derived from the third order equation

$$y^3 + \frac{(|\epsilon|^4 - 3|\epsilon|^2)}{(2|\epsilon|^2 + 2\epsilon_1)} y^2 - \frac{|\epsilon|^4}{(|\epsilon|^2 + \epsilon_1)} y + a = 0 \quad (2)$$

with $y = \sin^2 \phi_B$ and $a = |\epsilon|^4 / (2|\epsilon|^2 + 2\epsilon_1)$. The solution is straightforward and will be given elsewhere.²⁴ The corresponding equation for the reflectivity, R_p , is developed from the Fresnel equations:

$$R_p = r_p r_p^* = \frac{\mu + |\epsilon|^2 \cos^2 \phi - \cos \phi (\mu + \sin^2 \phi) \sqrt{2(\mu + \kappa)}}{\mu + |\epsilon|^2 \cos^2 \phi + \cos \phi (\mu + \sin^2 \phi) \sqrt{2(\mu + \kappa)}} \quad (3)$$

$$\mu^2 = |\epsilon|^2 - 2\epsilon_1 \sin^2 \phi + \sin^4 \phi \quad \text{and} \quad \kappa = \epsilon_1 - \sin^2 \phi. \quad (4)$$

ϕ denotes the angle of incidence.

¹ D. V. Lang, J. Appl. Phys. 45, 3023 (1974).

² R. Langfeld, Appl. Phys. A 44, 107 (1987).

³ S. Makram-Ebeid and P. Boher, Rev. Phys. Appl. 23, 847 (1988).

⁴ A. Schary and C. A. Lee, J. Appl. Phys. 67, 200 (1990).

⁵ M. Kaminska, Rev. Phys. Appl. 23, 793 (1988).

⁶ R. Haak and D. Tench, J. Electrochem. Soc. 131, 275 (1984).

⁷ B. Dischler and U. Kaufmann, Rev. Phys. Appl. 23, 779 (1988).

⁸ J. W. Garland, H. Abad, M. Viccaro, and P. M. Raccach, Appl. Phys. Lett. 52, 1176 (1988).

⁹ M. Gal and C. Shwe, Appl. Phys. Lett. 56, 545 (1990).

¹⁰ E. G. Bylander, C. W. Myles, and Y.-T. Shen, J. Appl. Phys. 67, 7351 (1990).

¹¹ J. Schneider, Mat. Res. Soc. Symp. Proc. 14, 225 (1983).

¹² B. K. Meyer, J.-M. Spaeth, and M. Scheffler, Phys. Rev. Lett. 52, 851 (1984).

¹³ B. K. Meyer, Rev. Phys. Appl. 23, 809 (1988).

¹⁴ S. K. Brierley and D. S. Lehr, J. Appl. Phys. 67, 3878 (1990).

¹⁵ D. Fournier and A. C. Boccara, Mat. Sci. Eng. B 5, 83 (1990).

¹⁶ T. S. Moss, *Optical properties of semiconductors* (Butterworths, London, 1959).

¹⁷ K. W. Böer, *Survey of Semiconductor Physics: Electrons and other Particles in Bulk Semiconductors* (Van Nostrand Reinhold, New York, 1990).

¹⁸ I. N. Bronstein and K. A. Semendjajew, *Taschenbuch der Mathematik*, 19th ed. (Verlag Harri Deutsch, Frankfurt/Main, 1980) p. 826.

¹⁹ J. C. Bourgoin and H. J. v. Bardeleben, J. Appl. Phys. 64, R65 (1988).

²⁰ B. A. Lombos, T. Bretagnon, A. Jean, R. L. V. Mao, S. Bourassa, and J. P. Dodelet, J. Appl. Phys. 67, 1879 (1990).

²¹ M. O. Manasreh, D. W. Fischer, and W. C. Mitchel, Phys. Status Solidi (B) 154, 12 (1989).

²² L. Eaves, A. W. Smith, S. M. S., and B. Cockayne, J. Appl. Phys. 53, 4955 (1982).

²³ S. P. F. b. t. l. Humphreys-Owen, Proc. Phys. Soc. 77, 949 (1961).

²⁴ N. Dietz and H. J. Lewerenz (unpublished).